AIAA SciTech
4-8 January 2016, San Diego, California, USA
57th AIAA/ASCE/AHS/ASC Structures, Structural Dynamics, and Materials Conference

CrossMark
click for updates

Nanoparticle Alignment using Oscillating Magnetic Fields for Scalable Nanocomposite Manufacturing

Mychal P. Spencer[1] and Namiko Yamamoto[2]
The Pennsylvania State University, University Park, PA, 16802

Magnetic assembly is a promising, scalable nanomanufacturing method to organize nanofillers within polymer nanocomposites. Nanocomposites, tailorable multifunctional materials, are critical for the advancement of aerospace technologies because nanocomposites can be potentially engineered to function for long operation endurance with light-weight, structural integrity, high thermal and radiation stability, and even with actuation/morphing capabilities. However, nanocomposite application is currently limited due to poor scalability; bulk fabrication of nanocomposites with high-quality nanostructures leading to high performance characteristics is missing. Here an active assembly of nanofillers using oscillating magnetic fields is studied to evaluate its effectiveness of organizing nanofillers throughout large-size nanocomposites. The approach taken is to parametrically study how the frequency and the flux density of the applied magnetic field influence the alignment of superparamagnetic iron oxide particles. In this parametric study, the capability to control particle alignment geometry, including the alignment line separation, is demonstrated; the effectiveness of oscillating magnetic fields to align particles is confirmed even with weak fields or 10-100 G, and particularly with small frequencies of 0.1-5 Hz. The alignment line separation increases by an average 50% when the frequency is increased from 0 Hz (DC) to 1.0 Hz with a magnetic flux density of 50-100 G. The width of the alignment lines shows an ~20% increase with low frequency ranges up to 0.1 Hz, but plateaued beyond 1 Hz. The length of the alignment lines between 50-100 G increases by an average 60% for low frequencies at or below 0.1 Hz, but show a decreasing trend for frequencies greater than 0.1 Hz. Knowledge obtained based on this study is expected to lead to a better understanding of nanoparticle alignment with the goal of coupon-sized nanocomposites with tailored and consistent nanoparticle structures in the future.

Downloaded by PENNSYLVANIA STATE UNIVERSITY on August 26, 2016 | http://arc.aiaa.org | DOI: 10.2514/6.2016-0150

Nomenclature

K	=	anisotropy energy density
k_B	=	Boltzmann constant
T	=	temperature
τ_o	=	time constant
V	=	particle volume

I. Introduction

MULTI-FUNCTIONAL polymer nanocomposites are recognized as a critical research topic because these materials are essential for lower-cost, low-mass and more efficient aerospace design.[1] Through micro-structure design, and with the proper choice of components, the properties of nanocomposites can be tailored to have high mechanical rigidity or flexibility,[2] mechanical actuation,[3] thermal insulation or stability,[4] radiation shielding,[5] and more.[6,7] However, bulk application of nanocomposites is currently not feasible because scalable manufacturing is missing to produce large-sized nanocomposites while maintaining organized microstructures. In the past, nanoparticles were directly mixed in polymers; nanoparticle distribution in the polymers was nonhomogeneous, and thus properties improved marginally or even degraded.[8-10] In order to achieve bulk but controlled nanoparticle organization in nanocomposites, particle assembly using oscillating magnetic fields is investigated in this work.

[1] Graduate Research Assistant, Aerospace Engr., 229 Hammond, University Park, PA 16802, Student Member
[2] Assistant Professor, Aerospace Engineering, 232A Hammond, University Park, PA 16802, Member

Copyright © 2015 by the American Institute of Aeronautics and Astronautics, Inc. All rights reserved.

Active assembly using oscillating magnetic fields is a promising scalable nanomanufacturing method because it allows for the bulk processing of nanocomposites while maintaining high periodicity and patterning capability. The magnetic assembly of particles has been studied in the past, but knowledge gaps exist to achieve controlled bulk assembly of nanoparticles. In the past, the response of ferromagnetic nanoparticles in solutions against external, *static* (DC) magnetic fields has been quantitatively evaluated through analytical and experimental studies, together with other effects including particle-to-particle magnetic interactions and thermal fluctuations.[11] An example of previous studies using DC magnetic fields includes the usage of ferromagnetic materials within the human body for detection, separation, and treatment of cells.[11-14] Also, the active and effective alignment of *bulk* microparticles (rods, platelets, etc.) has been studied in the past using oscillating magnetic fields to fabricate particle-polymer composites with organized microstructures leading to novel mechanical properties.[15-18] These studies prove that effective microplatelet assembly, with optimized particle geometry and magnetic properties, can be obtained using very small (~1 mT, an order of magnitude above the earth's natural magnetic field) and oscillating magnetic fields.[19] Although the previous studies demonstrated the effective assembly of nano-particles with *static* magnetic fields and also of microparticles with oscillating magnetic fields, the understanding of some critical issues on how *nano*particles are assembled with *oscillating* magnetic fields is missing: the nano-size effects, particle-to-particle and solvent-to-particles interactions, and the maximum size of microstructures that can be processed.

Our work focuses on nanoparticle assembly using oscillating magnetic fields to understand and control nanoparticles movements in solutions, and then to eventually achieve coupon-sized nanocomposites with tailored and consistent nanoparticle structures, as described in Fig. 1. As a model case, we quantitatively study the response of superparamagnetic iron oxide nanoparticles in water when exposed to oscillating magnetic fields generated between a pair of solenoids. When a magnetic field is applied, the superparamagnetic particles form a collection of linear clusters aligned in the direction of the magnetic field. The nanoparticle concentration, along with the frequency and amplitude of the applied magnetic field, are varied and real-time images are collected to observe the effect on alignment of the iron oxide particles. The resulting images are processed using algorithms to evaluate alignment: number of *clusters*, and linear cluster geometries (width, length, and separation between linear clusters). As described in Fig. 1, these experimentally observed behaviors will be compared with analytical studies in the future to identify key parameters and their ranges that determine nanoparticle structuring; this novel knowledge on magnetic assembly of nanoparticles will be directly applied to scalable nanocomposites and their microstructure designs.

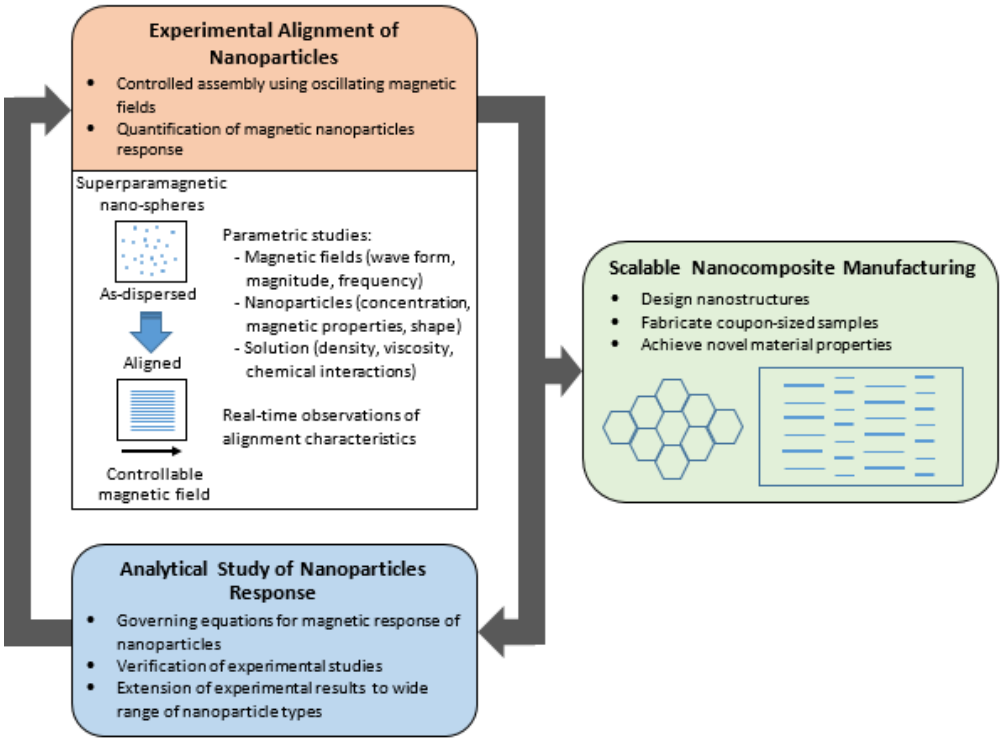

Figure 1. Research overview to achieve scalable patterning of nanoparticles.

Downloaded by PENNSYLVANIA STATE UNIVERSITY on August 26, 2016 | http://arc.aiaa.org | DOI: 10.2514/6.2016-0150

II. Materials and Methods

A. Nanoparticle Solution

Spherical, superparamagnetic iron oxide particles (Sigma-Aldrich I7643) supplied in an aqueous suspension (50 mg per ml in 1 mM EDTA, pH 7.0) are used in this work; the particles are amine-terminated to maintain particle suspension. These nano-sized particles deliver unique superparamagnetic properties because, at very small particle sizes (on the order of tens of nanometers),[20] the magnetic moment of a particle will randomly change direction due to thermal energy.[21] The time between changes in direction of the magnetic moment is approximated using Néel's model as shown in Eq. (1), where V is the particle volume (m^3), T is the temperature (K), k_B is Boltzmann constant (m^2 kg s^{-2} k^{-1}), τ_o is a time constant (~10^{-9}-10^{-10}),[20-21] and K is the anisotropy energy density (~13500 10^4 J/m^3 for magnetite at room temperature).[24] Superparamagnetic particles are characterized as having a relaxation time at or below 10^{-1} s.[22]

$$\tau = \tau_o \exp\left(\frac{KV}{k_B T}\right) \tag{1}$$

Transmission electron microscopy (TEM) images of the particle size and clusters are shown in Fig. 2; particle sizes were observed to be between ~10 nm and ~20 nm, and particle clusters were observed to be between ~1 μm and ~10 μm in length. The clusters are roughly homogeneous in shape, as observed by the microscope in Fig. 3. Using spherical particle sizes of 10 nm and 20 nm, the range of relaxation time is calculated to be between ~10^{-3} and 10^{-9} seconds indicating superparamagnetic behavior. It is hypothesized that the clusters form due to a combination of van der Waals forces, electrostatic potential, and/or chemical interactions. Due to the superparamagnetic behavior of the particles, magnetic interactions are not expected between the particles and/or clusters without an external magnetic field.

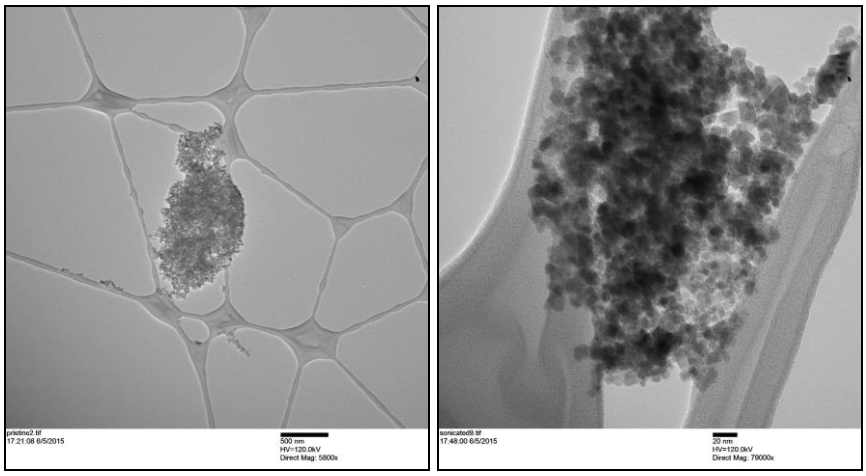

Figure 2. TEM images of superparamagnetic iron oxide clusters. The scale bar for the left image is 500 nm and for the right image is 20 nm.

The magnetic properties of the iron oxide particle solution are characterized using a vibrating sample magnetometer (MicroSense Vibrating Sample Magnetometer) as shown in Fig. 4. A solution concentration of 4 mg/ml is housed in a container of volume 6.77x10^{-2} ml. The solution container is inserted between the solenoid coils, and is then vibrated in a uniform magnetic field. The induced magnetic flux is proportional to and obtained through the induced voltage measured by the detection coils. The M-H magnetic response of these superparamagnetic particles was measured to be anhysteretic due to the reversal of the magnetic moment.[20] The magnetic saturation is approximately 20.6 emu/g and the magnetic susceptibility is 0.61, in agreement with Schnyder and Pouliquen et al.[22,25]

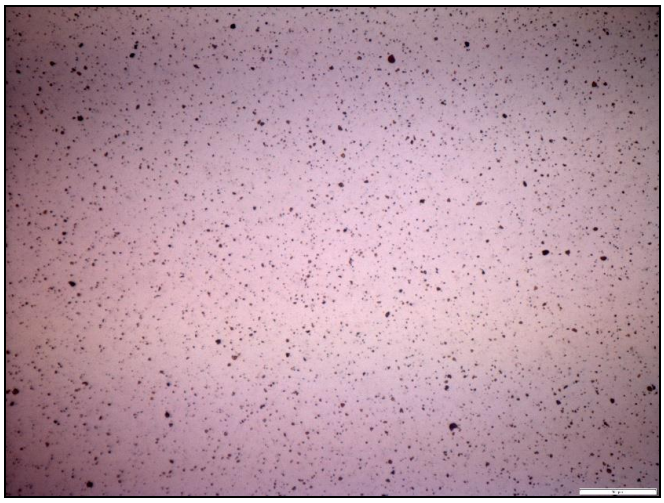

Figure 3. Microscope image showing the distribution of superparamagnetic iron oxide clusters in deionized water (2 mg/ml). The scale bar is 100 μm.

Downloaded by PENNSYLVANIA STATE UNIVERSITY on August 26, 2016 | http://arc.aiaa.org | DOI: 10.2514/6.2016-0150

Downloaded by PENNSYLVANIA STATE UNIVERSITY on August 26, 2016 | http://arc.aiaa.org | DOI: 10.2514/6.2016-0150

B. Experimental Set-up

The iron oxide suspension is diluted using deionized (DI) water to the concentration of 2 mg per ml. The solution is encapsulated in a KOVA Glasstic slide with a height of 0.1 mm and a chamber volume of 6.6 µl, and then is mounted between a pair of solenoids. With the solenoid pair (570 turns, 14.8 cm length, 6.51 cm inner diameter, 16 gauge enameled wire, 410 stainless steel core) in series, a maximum magnetic flux density of ~100 G is produced at a separation distance between the solenoids of 10.2 cm. The current is supplied to the solenoid pair by a KEPCO BOP 20-10M bipolar power supply (200 W, ±20 V, ±10 A) which is driven by a BK Precision 4014B function generator capable of producing square, sine, and triangle waveforms. The magnetic flux density is measured using a LakeShore Model 425 gaussmeter in conjunction with a BK Precision 5105B oscilloscope. Real-time images of the patterning of the magnetic nanoparticles are captured using an Olympus BX51WI digital microscope. The magnetic field is applied for a total of 15 minutes to ensure alignment saturation. Images are taken prior to the magnetic field being applied and at 5 and 10 minutes. A 50% duty cycle square waveform with magnetic flux density amplitudes of ±10 G, ±50 G, and ±100 G is used. Low frequencies are investigated (DC/0 Hz, 0.1 Hz, 1.0 Hz, and 5.0 Hz) based on previous work in the literature.[19,26] A schematic and an image of the experimental set-up are described in Fig. 5.

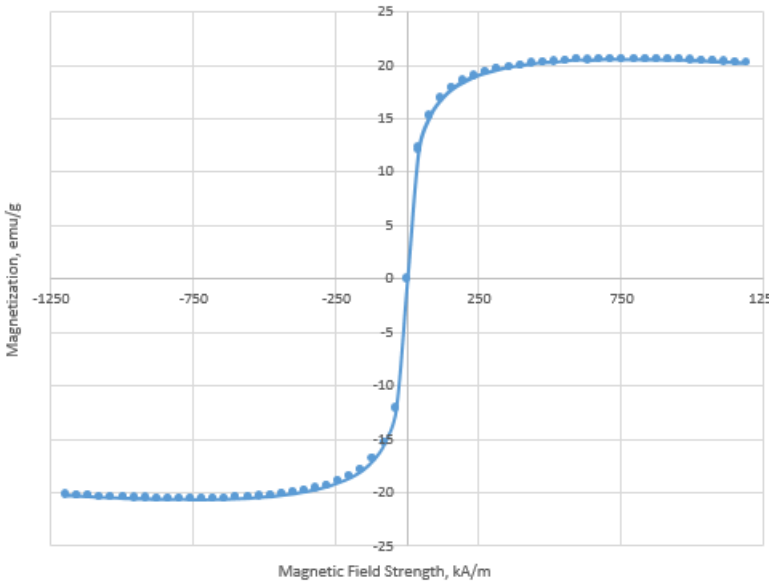

Figure 4. Magnetic hysteresis plot of superparamagnetic iron oxide particles (4 mg/ml). The applied magnetic fields are cycled from -1250 kA/m to 1250 kA/m, and then back to -1250 kA/m.

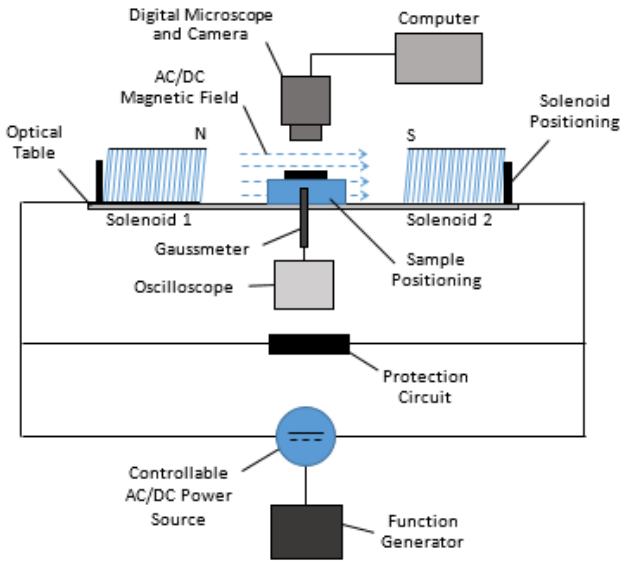

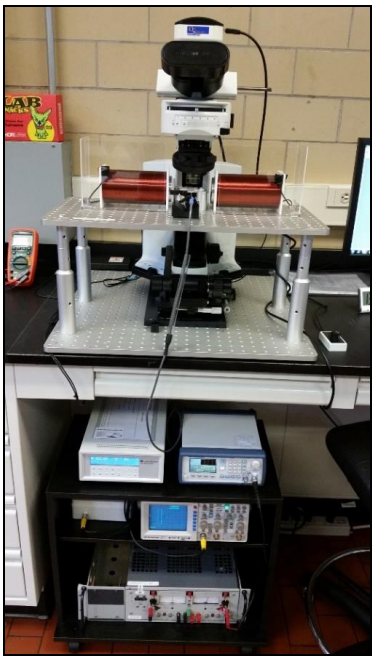

Figure 5. Experimental set-up for nanoparticle assembly using oscillating magnetic fields: schematic (left) and digital image (right).

Downloaded by PENNSYLVANIA STATE UNIVERSITY on August 26, 2016 | http://arc.aiaa.org | DOI: 10.2514/6.2016-0150

C. Image Processing

The microscope images are processed using analysis codes in Matlab to quantitatively evaluate particle morphology. The images are processed using the following procedure:

i. The image is converted to grayscale.
ii. The center region of the image is extracted due to a circular lensing effect near the edges of the image.
iii. The image is partitioned and a threshold is selected for each partition based upon the standard deviation of the grayscale pixel intensity values in the partition.
iv. The partitioned thresholds are recombined and Gaussian smoothing is applied to the overall threshold matrix.
v. The threshold matrix is applied to the original grayscale image to produce a black and white image.
vi. Each cluster is assigned a numerical label and clusters below a specified size are removed (to correct for thresholding artifacts – typically at or less than 20% of the mean cluster size).
vii. Each cluster is stored into an array and the size, width, and length is calculated, in addition to the separation between clusters.
viii. The results are converted into nm and output.

Example images of the analysis process are shown in Fig. 6. The left image shows the original magnetic nanoparticle solution with no applied magnetic field. When the magnetic field is applied, the nanoparticles form alignment patterns consisting of clusters. As shown in the right image, the algorithm outputs the cluster density and average size, length, width, and separation of the clusters.

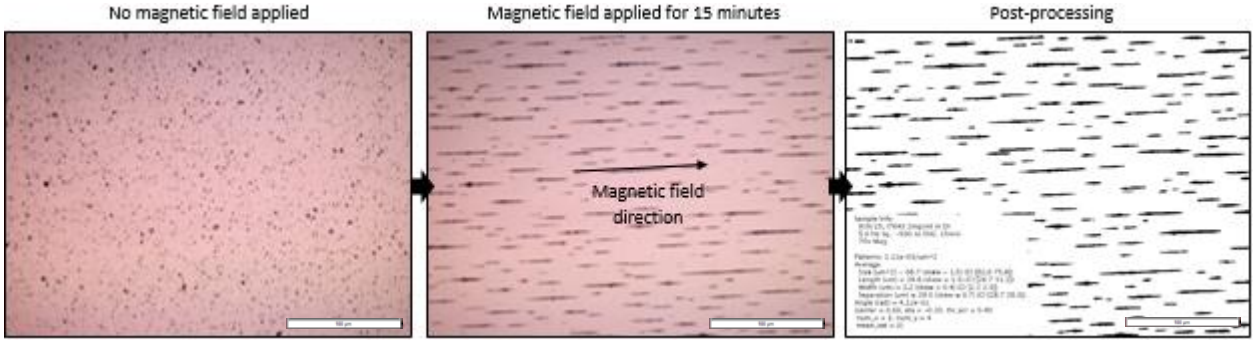

Figure 6. Microscope images showing mangetic alignment and image processing: original nanoparticle solution (left), and nanoparticles aligned with oscillating magnetic field (microscope image, center, and processed image, right). The scale bar is 100 μm.

III. Results and Discussion

A. Verification of Algorithm

Due to slight shadowing around clusters, the algorithm reproduces clusters at a slightly larger size; in all cases the algorithm produced slightly longer cluster lengths with an average error of approximately 3%. A comparison is made between the original cluster lengths and the cluster lengths output by the algorithm for three clusters at 10 G and 0.1 Hz, see Fig. 7.

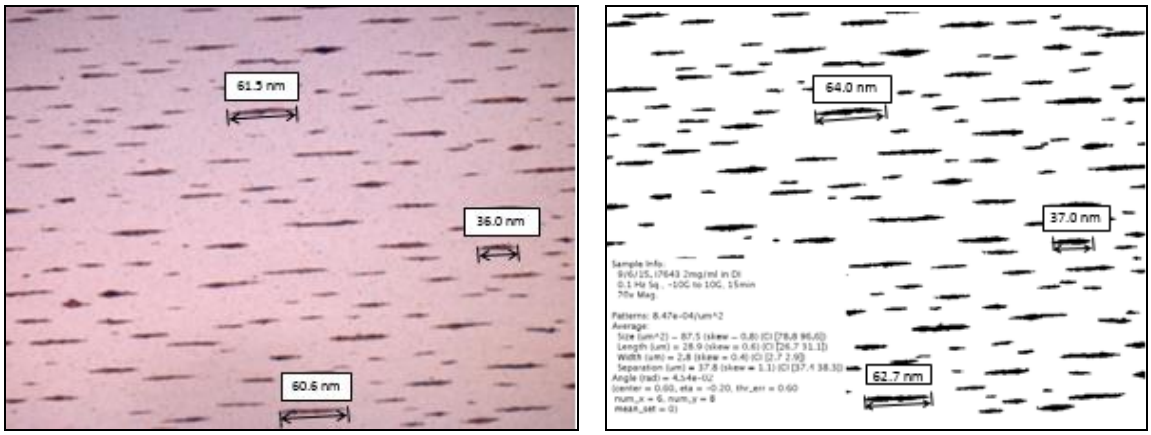

Figure 7. Verification of cluster length calculation by comparing the original clusters (left) with the output algorithm results (right).

Downloaded by PENNSYLVANIA STATE UNIVERSITY on August 26, 2016 | http://arc.aiaa.org | DOI: 10.2514/6.2016-0150

B. Discussion on Nanoparticle Assembly

The nanoparticle clusters are characterized based upon four primary metrics: the average length, the average width, the average separation, and the density. Each metric is evaluated as a function of two parameters: magnetic flux density (10 G, 50 G, and 100 G) and frequency (DC/0 Hz, 0.1 Hz, 1.0 Hz, and 5.0 Hz). The results show a clear dependency of the alignment patterns on the frequency and magnetic flux density, as depicted in Fig. 8, Fig. 9, Fig. 10, and Fig. 11.

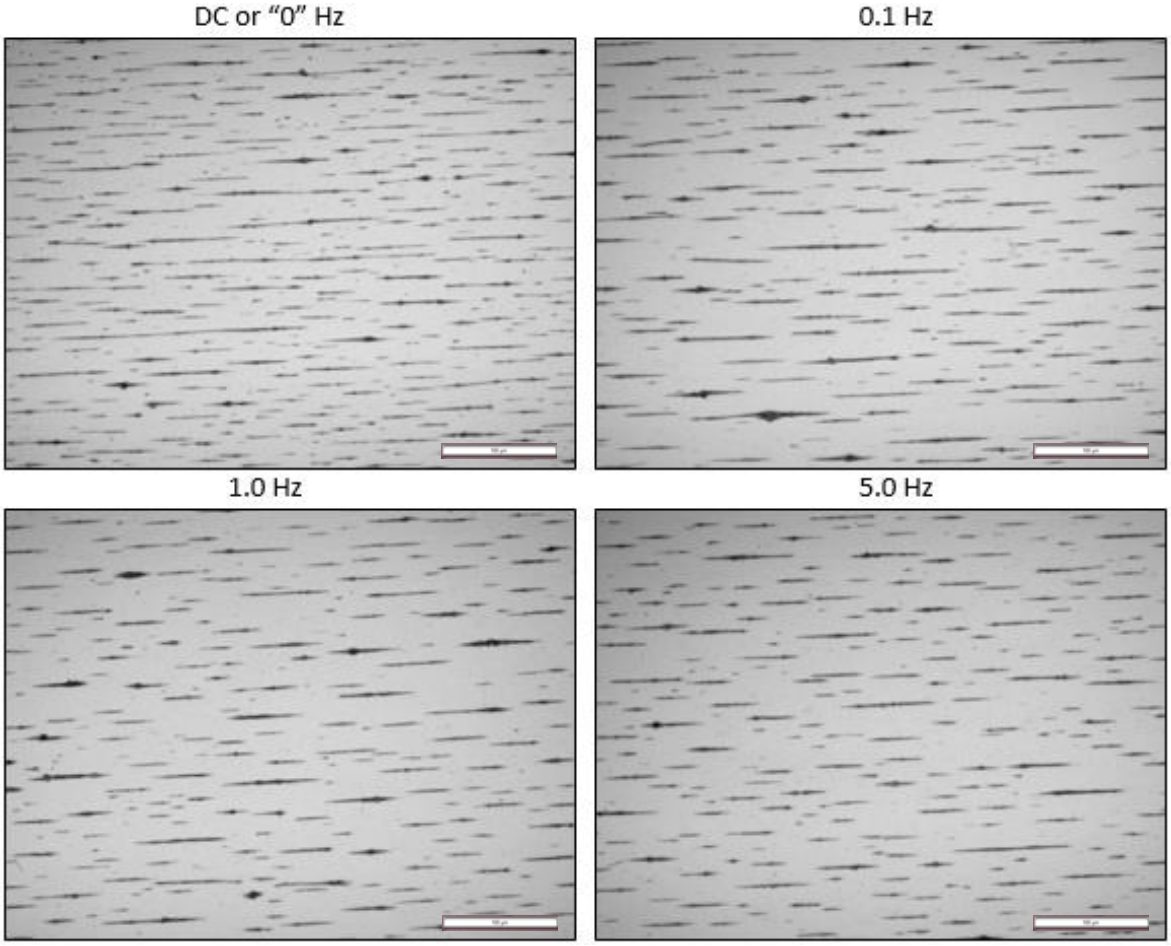

Figure 8. The microscope images of aligned nanofillers showing the effect of *frequency* on cluster agglomeration. The magnetic flux density applied is 50 G. The scale bar is 100 μm.

The particles and clusters are being acted upon primarily by four effects: the applied magnetic field, thermal energy, particle-to-particle interactions (e.g. van der Waals, magnetic interactions, etc), and hydrodynamics (due to viscosity of polymer matrices). While not shown, upon removal of the magnetic field the clusters immediately disperse indicating that the clusters, consisting of superparamagnetic nanoparticles, retain no net remnant magnetization. In addition, due to the dispersion of the clusters, it can be hypothesized that additional van der Waals and electrostatic interactions between particles are not responsible for cluster agglomeration as observed in Fig. 8 and Fig. 9, except for the initial particle agglomeration shown in Fig. 3. The thermal effects are also hypothesized to be neglible due to the size of the clusters (~1 μm or greater). In this work, the solution is deionized water and thus with low viscosity, so the effect of the hydrodynamics is also expected to be low. Therefore, cluster agglomeration is primarily controlled by the applied magnetic field and induced cluster-particle magnetic interactions.

First, the effect of the frequency of the oscillating magnetic field will be discussed (see Fig. 8 and Fig. 10). When the frequency is increased from 0 Hz (DC) to 0.1 Hz, longer, wider, and more separated nanoparticle clusters are formed, and thus the number of nanoparticle clusters per unit area is decreased. Meanwhile, when the frequency increases beyond 0.1 Hz and up to 5 Hz, the average cluster width and separation plateau and stay constant beyond 0.1 Hz, while the cluster length decreases up to and then plateaus at 1.0 Hz. It should be noted that all the pattern features (length, width, separation, and cluster density) exhibit the steepest changes at the low frequency range,

especially between DC and 0.1 Hz. Care should be exercised when interpreting the 10 G data; particles (cluster agglomerates less than <1 μm in size) are not sufficiently magnetized to be attracted to larger clusters and thus are not captured by the algorithm – this is discussed further in the following paragraph. These propensities can possibly be explained by considering the two main forces acting on the clusters: the magnetic moment due to the external magnetic field and the cluster-to-particle magnetic interactions. When the magnetic field is applied, magnetic moments are induced within the particles, as a collection of magnetic moments of nanoparticles within the particles, along the field direction. When the applied field is large enough (>10G), the particles will move along the field direction until they reach the vicinity of other particles or clusters and then adhere to them due to cluster-to-particle magnetic interactions(/attractions). Thus, in the case of a static (DC) field, the formed clusters are aligned along the applied field, and come in a variety of lengths with a relatively short average (see Fig. 8), as the particles will adhere to any other particles/clusters that come in their vicinity first. Meanwhile, when the magnetic field is oscillating, the particles will have a chance to detach from clusters and travel further, forming longer, wider, and more separated clusters. This particle detachment behavior should require a large enough magnetic field such that the induced magnetic moment is larger than the cluster-to-particle magnetic attractions, and also potentially requires enough time for the particles to react against the switching of magnetic moment directions. This hypothesis is compatible with observation that the cluster length, width, and separation plateau at higher frequencies. These results demonstrate that the magnetic field frequency has the capability to control nanofiller alignment pattering for nanocompositing - this includes the cluster separation, which is critical in tailoring nanocomposite properties and increases by an average ~50% from DC up to 1.0 Hz for 50-100 G.

Downloaded by PENNSYLVANIA STATE UNIVERSITY on August 26, 2016 | http://arc.aiaa.org | DOI: 10.2514/6.2016-0150

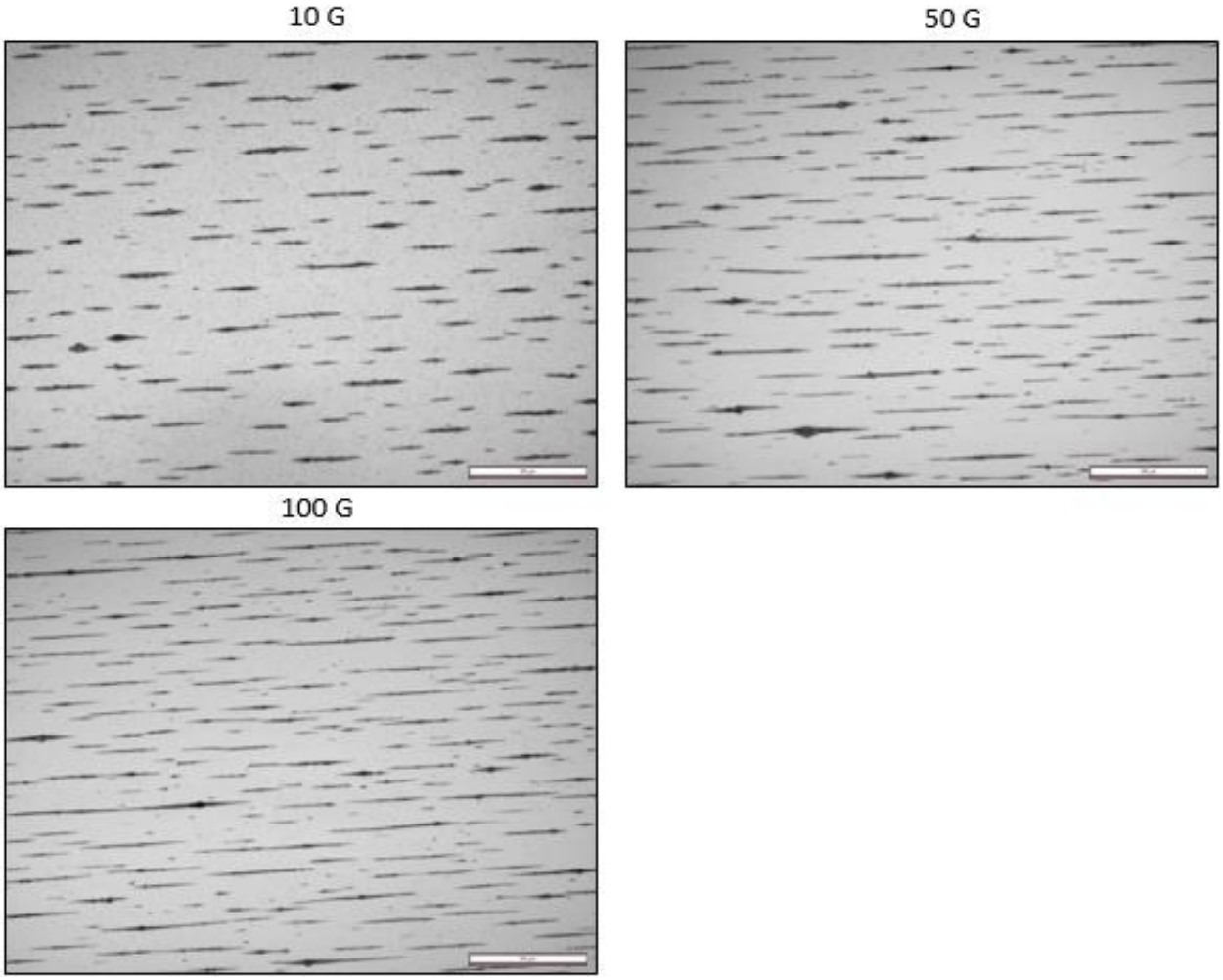

Figure 9. The microscope images of aligned nanofillers showing the effect of *magnetic flux density* on cluster agglomeration. The magnetic field frequency is 0.1 Hz. The scale bar is 100 μm.

Downloaded by PENNSYLVANIA STATE UNIVERSITY on August 26, 2016 | http://arc.aiaa.org | DOI: 10.2514/6.2016-0150

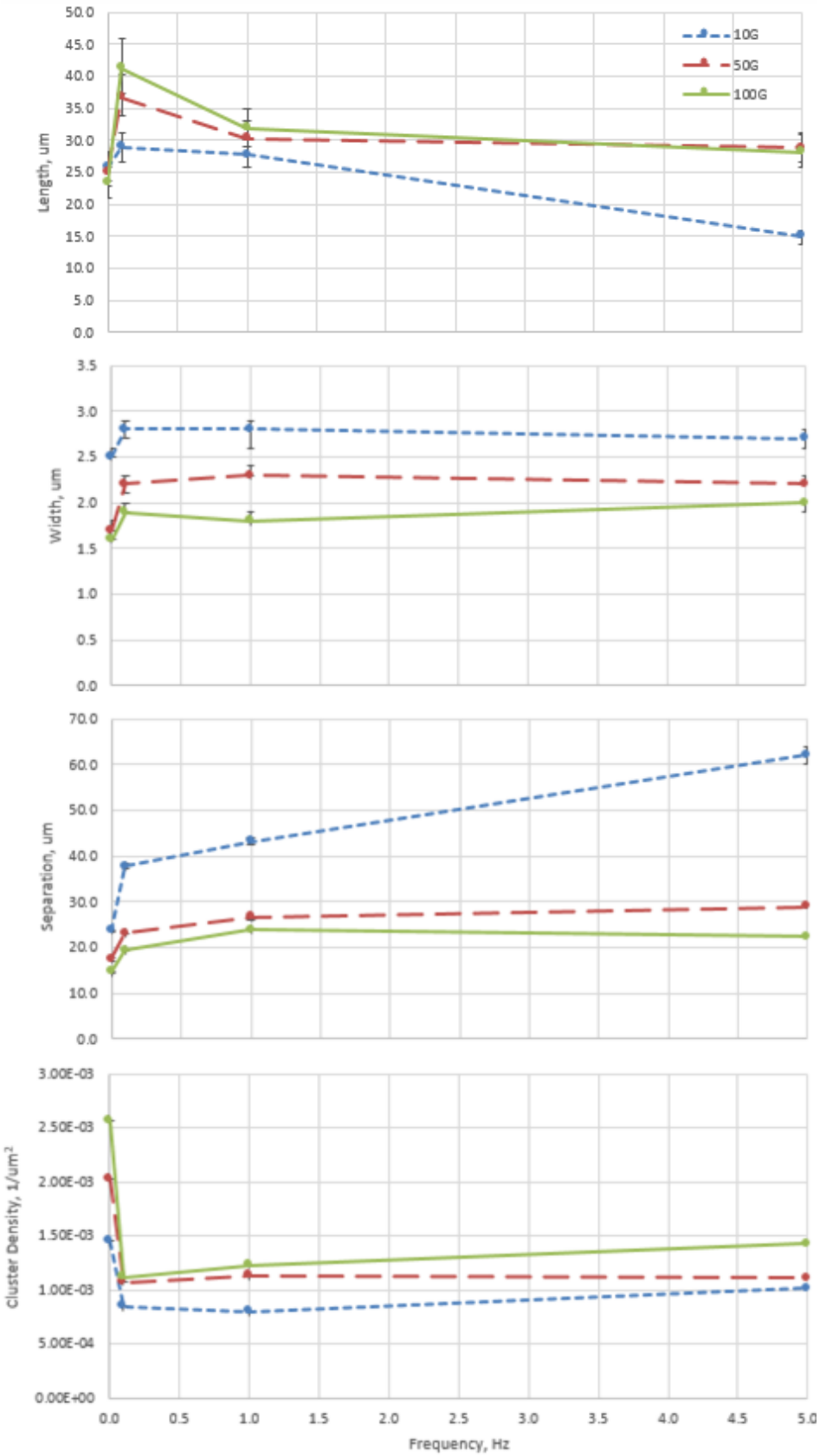

Figure 10. Particle assembly (cluster) geometries as a function of *frequency*: (from top to bottom) average cluster lengh, width, separation, and density.

Downloaded by PENNSYLVANIA STATE UNIVERSITY on August 26, 2016 | http://arc.aiaa.org | DOI: 10.2514/6.2016-0150

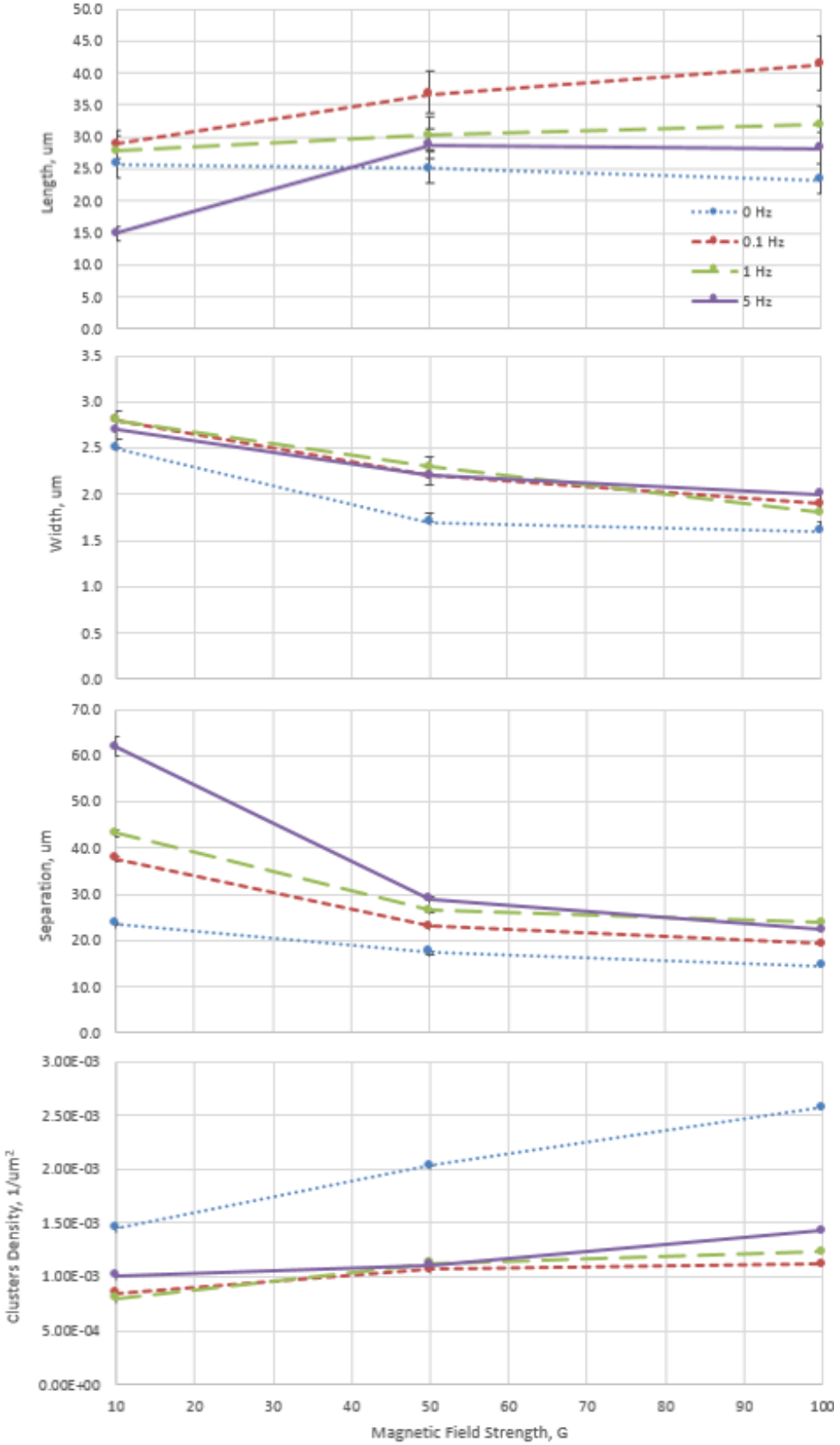

Figure 11. Particle assembly (cluster) geometries as a function of *magnetic flux density*: (from top to bottom) average cluster lengh, width, separation, and density.

Second, the effect of the magnetic flux density will be discussed (see Fig. 9 and Fig. 11). With increasing magnetic flux density, thinner and less separated clusters are formed, leading to a slight increase in the number of nanoparticle clusters per unit area. As shown in Fig. 9, with the low magnetic field of 10 G, particles (cluster agglomerates <~1 μm in size, which make the image appear 'grainy') are observed, together with larger clusters, because the induced magnetic moments are not large enough to move the particles; the threshold magnetic flux density resides between 10 to 50 G to align these particles. In addition, due to the small size, these particles are not captured by the image processing algorithm. Thus, although the processed data for the case where the magnetic flux density of ~ 10G is given in Figure 11, this discussions focuses on the data for the cases where the magnetic flux density is 50 G and 100 G, for a fair comparative study. The average cluster length is approximately constant (slight increase) regardless of the magnetic flux density (50 or 100 G), indicating that the cluster length is primarily a function of the frequency. Similarly, the cluster width and separation show only a slight decrease between 50 and 100 G. For increasing magnetic flux density, the magnetic moments applied to the clusters increases which tends to elongate the clusters along the magnetic field direction – this leads to a slight reduction in the average cluster width, and a slight increase in the average cluster length.

Variations in the alignment patterns due to changes in the magnetic flux density are smaller than those found due to changes in the magnetic field frequency, especially for the low frequency range. This trend can be explained by considering that frequency changes the direction of the magnetic moment while the magnetic flux density only sets the threshold for the magnitude of the magnetic moment required to counteract against the cluster-to-particle attractions. In other words, the magnetic field strength is a useful parameter for making minor modifications to the alignment characteristics.

IV. Conclusion

The goal of this work is to better understand the alignment characteristics of iron oxide nanoparticles exposed to oscillating magnetic fields, which will assist in enabling scalable manufacturing of tailored nanocomposites through active assembly of nanofillers. The frequency, particularly in the low range (~0.1 Hz) was confirmed to be the effective parameter to determine the alignment characteristics, including the linear cluster separation, rather than the magnetic flux density. This trend can be explained with the hypothesis that the nanoparticle movements were controlled by the two main forces: the magnetic moment due to the external field and the cluster-to-particle magnetic interactions. Effective control of nanoparticles with low frequencies requires less power and is thus advantageous. Future work will include studying nanoparticle alignment in polymer matrices and thus of hydrodynamic moment, investigating the effect of gravity, evaluation of the alignment patterns over large regions of the samples, scaling up the assembly to produce larger samples, and verifying the experimental results with analytical studies.

Acknowledgments

The authors would like to thank T. Clark and J. Gray from the Materials Characterization Lab at PSU for their assistance with TEM and SEM, and also thank Dr. vonLockette and C. Breznak for assistance with VSM measurements. This work is supported by the Pennsylvania State University, Department of Aerospace Engineering, and the Hartz Family Career Development Professorship in Engineering.

References

[1]Meador, M.A., Files, B., Li, J., Manohara, H., Powell, D., and Siochi, E.J., "NASA Nanotechnology Roadmap – Technology Area 10," NASA, 2012.

[2]Mansoori, G.A., "Advances in Atomic and Molecular Nanotechnology," In Nanotechnology: The emerging cutting-edge technology, UN-APCTT Tech Monitor, 2002, pp. 53-59.

[3]Ahir, S.V. and Terentjev, E.M., "Photomechanical Actuation in Polymer-Nanotube Composites," Nature Materials 4, 2005, pp. 491-495.

[4]Yamamoto, N., Gdoutos, E., Toda, R., White, V., Manohara, H., and Daraio, C., "Thin Films with Ultra-Low Thermal Expansion," Adv. Mater. 26, 2014, pp. 3076-3080.

[5]"National Nanotechnology Initiative – Leading to the Next Industrial Revolution," Microscale Thermophysical Engineering, 2010, pp. 205-212.

[6]Pulickel, M.A., Schadler, L.S., and Braun, P.V., *Nanocomposite Science and Technology*, Wiley-VCH, Weinheim, Germany, 2003.

[7](Editors) Chou, T.W. and Sun, C.T., "Series on Advances in Composite Materials Volume 2: Nanocomposites," Am. Soc. for Composites, DEStech Publications, Lancaster, PA, 2012.

[8]Thostenson, E.T., Li C., and Chou, T-W., "Review – Nanocomposites in Context," Comp. Sci. Tech. 65, 2005, pp. 491-516.

Downloaded by PENNSYLVANIA STATE UNIVERSITY on August 26, 2016 | http://arc.aiaa.org | DOI: 10.2514/6.2016-0150

[9]Moniruzzaman, M. and Winey, K.I., "Polymer Nanocomposites Containing Carbon Nanotubes," Macromolecules 39, 2006, pp. 5194-5205.
[10]Song, Y.S. and Youn, J.R., "Influence of Dispersion States of Carbon Nanotubes on Physical Properties of Epoxy Nanocomposites," Carbon 43, 2005, pp. 1378-1385.
[11]Valberg, P.A. and Butler, J.P., "Magnetic Particle Motions Within Living Cells – Physical Theory and Techniques," J. Biophysical Soc. 52, 1987, pp. 537-550.
[12]Yellen, B.B., Erb, R.M., Son, H.S., Hewlin, R., Shange, H., and Lee, G.U., "Traveling Wave Magnetophoresis for High Resolution Chip Based Separations," Lab Chip 7, 2007, pp. 1681-1688.
[13]Miltenyi, S., Muller, W., Weichel, W., and Radbruch, A., "High Gradient Magnetic Cell Separation With MACS," Cytometry 11, 1990, pp. 231-238.
[14]Jordan, A., Scholz, R., Wust, P., Fahling, H., and Felix, R., "Magnetic Fluid Hyperthermia (MFH): Cancer Treatment with AC Magnetic Field Inducted Excitation of Biocompatible Superparamagnetic Nanoparticles," J. Magnetism and Magnetic Mat. 201, 1998, pp. 413-419.
[15]Libanori, R., Erb, R.M., and Studart, A.R., "Mechanics of Platelet-Reinforced Composites Assembled Using Mechanical and Magnetic Stimuli," ACS Appl. Mater. Interfaces 5, 2013, pp. 10794-10805.
[16]Erb, R.M., Segmehl, J., Charilaou, M., Loffler, J.F., Studart, A.R., "Non-Linear Alignment Dynamics in Suspensions of Platelets under Rotating Magnetic Fields," Soft Matter 8, 2012, pp. 7604-7609.
[17]Garmestani, H., Al-Haik, M.S., Dahmen, K., Tannenbaum, R., Li, D., Sablin, S.S., and Hussaini, M.Y., "Polymer-Mediated Alignment of Carbon Nanotubes under High Magnetic Fields," Adv. Mat. 15, 2003, pp. 1918-1921.
[18]Hong, C.Y., Horng, H.E., Kuo, F.C., Yang, S.Y., Yang, H.C., and Wu, J.M., "Evidence of Multiple States of Ordered Structures and a Phase Transition in Magnetic Fluid Films Under Perpendicular Magnetic Fields," App. Phy. Let. 75, 1999, pp. 2196-2198.
[19]Erb, R.M., Libanori, R., Rothfuchs, N., and Studart, A., "Composites Reinforced in Three Dimensions by Using Low Magnetic Fields," Science 335, 2012, pp. 199-204.
[20]Pankhurst, Q.A., Connolly, J., Jones, S.K., and Dobson, J., "Applications of Magnetic Nanoparticles in Biomedicine," J. Phys. D: Appl. Phys. 36, 2003, pp. R167-R181.
[21]Bowles, J., Jackson, M., Chen, A., and Solheid, P., "Interpretation of Low-Temperature Data Part 1: Superparamagnetism and Paramagnetism," IRM Quarterly, 19 (3), 2009.
[22]Schnyder, J-S. D., "Magnetic Characterization of Iron Oxide Nanoparticles," Thesis, Department of Earth Sciences, ETH Zürich, 2010.
[24]Gossuin, Y., Gillis, P., Hocq, A., Vuong, Q.L., and Roch, A., "Magnetic Resonance Relaxation Properties of Superparamagnetic Particles," WIREs Nanomed Nanobiotechnol 1, 2009, pp. 299-310.
[25]Pouliquen, D., Perroud, H., Calza, F., Jellet, P., and Le Jeune, J.J., "Investigation of the Magnetic Properties of Iron Oxide Nanoparticles Used as Contrast Agent for MRI," Mag. Reson. In Med. 24, 1992, pp. 75-84.
[26]Wirtz, D. and Fermigier, M., "One-Dimensional Patterns and Wavelength Selection in Magnetic Fields," Phys. Letter Rev. 72, 1994, pp. 2294-2297.

Downloaded by PENNSYLVANIA STATE UNIVERSITY on August 26, 2016 | http://arc.aiaa.org | DOI: 10.2514/6.2016-0150